ELSEVIER

International Journal of Mass Spectrometry 202 (2000) 351–361

International Journal of Mass Spectrometry

A flowing afterglow selected ion flow tube (FA/SIFT) comparison of SIFT injector flanges and $H_3^+ + N$ revisited

Daniel B. Milligan, David A. Fairley, Colin G. Freeman, Murray J. McEwan*

Department of Chemistry, University of Canterbury, Christchurch, New Zealand

Received 27 September 1999; accepted 1 June 2000

Abstract

The performances of two different but interchangeable Venturi injectors (an annulus and a hole injector) have been compared in a new flowing afterglow source-selected ion flow tube (FA/SIFT) instrument built at the University of Canterbury. The tests applied compared the relative "pumping efficiencies" of the two injectors; their ion transmission using (O_2^+); the relative ease of injecting cluster ions subject to collision induced dissociation ($H_3O^+ \cdot H_2O$); and the extent of isomerization of ions sensitive to structural changes during the injection process ($C_3H_5^+$). The annulus injector was clearly superior to the hole injector in pumping efficiency. Thereafter the improvement in performance was only marginal. The greater difficulty of construction and maintenance of the annulus injector needs to be balanced against the slightly less versatile hole injector. It was necessary to direct a significant fraction of the total helium buffer gas flow through an outer, noncritical orifice to maintain satisfactory performance in the hole injector when injecting ions susceptible to collision induced dissociation. Finally, the new instrument was used to reexamine the reaction of H_3^+ and N atoms, which was found to be a nonreactive system, $k < 5 \times 10^{-11}$ cm^3 s^{-1}. (Int J Mass Spectrom 202 (2000) 351–361) © 2000 Elsevier Science B.V.

Keywords: Selected ion flow tube (SIFT); Flowing afterglow; Venturi injector; N atoms; H_3^+

1. Introduction

The flowing afterglow (FA) technique, first used to investigate neutral–neutral reactions, was later successfully applied to ion–molecule chemistry by Ferguson and co-workers in the early 1960's [1]. One of the difficulties associated with the FA technique was its inability to produce a single reactant ion species in the flow tube. Smith and Adams developed the selected ion flow tube (SIFT) technique to help overcome the multiple reactant ion problem [2,3]. In the SIFT technique ions produced in a separate ion source are mass selected by a quadrupole mass spectrometer in the source region before injection into the reaction flow tube against a pressure gradient. The ion injection is accomplished using an injector flange utilizing a Venturi nozzle. This nozzle is vital to the SIFT technique because it allows ions selected by the quadrupole mass spectrometer to be extracted from a region of low pressure into a region of much higher pressure. The injector flange used by Smith and Adams consisted of an array of twelve 1-mm-diameter holes, equally spaced around a circle 20 mm in diameter [2,3].

Recently Fishman and Grabowski (FG) [4] examined the performance of such "hole injector" Venturi

* Corresponding author. E-mail: m.mcewan@chem.canterbury.ac.nz

PII S1387-3806(00)00263-3

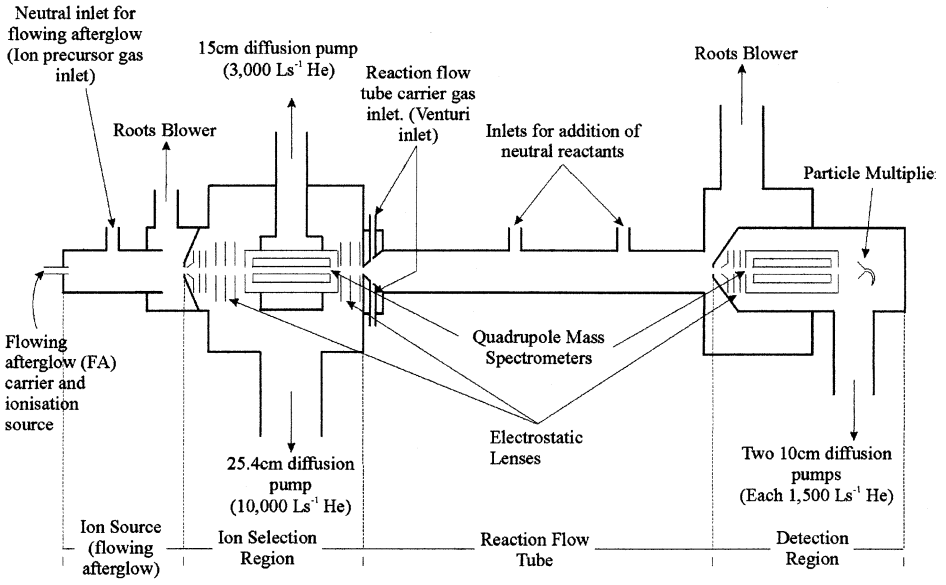

Fig. 1. Schematic of the FA/SIFT instrument at the University of Canterbury.

inlets by varying the diameter and the number of holes used. They also tried different geometries and examined the effect on performance of using an additional ring of 36, 1.4-mm-diameter holes around a 44.5-mm-diameter circle in order to gauge the influence of turbulence arising from the injection process. The FG study concluded that turbulence was not a problem for "hole injector" inlets. They also concluded that their best experimental data was obtained from an injector having 12, 0.2-mm-diameter holes on a planar surface where the holes were situated as closely as possible to the ion-entrance orifice. The injector with these characteristics was designated Pitt D in [4].

The main alternative to the "hole injector" Venturi is the "annulus" Venturi, which is somewhat more difficult to construct and to maintain. A number of these "annulus-type" Venturis have been built [5–8] with many of them utilizing a design (sometimes called the NOAA design [5]) in which the inlet wall slopes away from the ion inlet aperture and makes a 45° angle with the flow tube axis. The buffer gas enters the NOAA II Venturi [5] through a 0.025-mm-wide annulus that is concentric with the ion entrance aperture and has an internal diameter of 8.7 mm. The plane of the ion entrance aperture was 2.5 mm from the plane containing the annulus. Dupeyrat et al. [5] characterised the pumping efficiency of the "annulus" injectors whereas FG reported the same quantity for the "hole injector" [4].

The process of injecting an ion through an orifice against a pressure gradient requires the ion to drift through the orifice with a small but finite injection energy. This energy can be varied but even at its lowest values may still be sufficient to cause fragmentation of weakly bound ions. In this study we compare the extent of fragmentation for the two types of injector inlets using a new FA/SIFT instrument built in our laboratory. We also report the results of a reinvestigation of the H_3^+ + N atom reaction using the new instrument.

2. Experimental

The SIFT instrument previously used in our laboratory has been described earlier [9]. This equipment has since been extensively modified by the addition of a FA ion source and the incorporation of much larger pumping capacity than was present in the original instrument. A diagram of the new apparatus is given

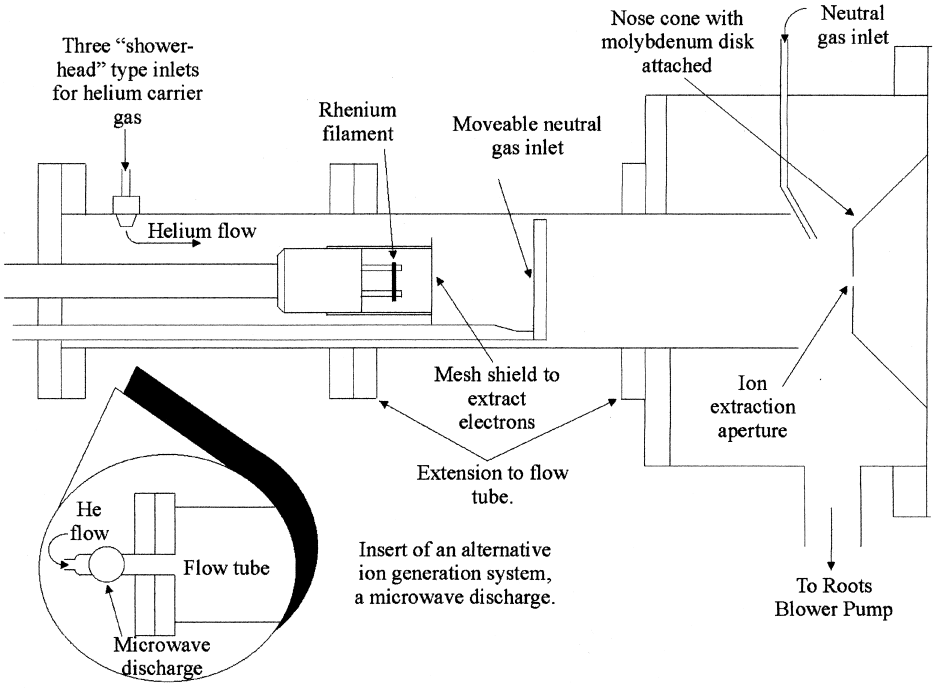

Fig. 2. Diagram of the FA source flow tube.

in Fig. 1. A drift tube, which has been described previously [10], can be inserted into the reaction flow tube but is not used in the present study.

The new FA source is similar in principle to that described by Van Doren et al. [11] and consists of a 20.5-cm-long flow tube [4.8 cm inner diameter (i.d.)] welded inside to a 15.24 cm Tee section that contains a pumping port for an Edwards EH 1200 Roots pump backed by an Edwards E2M 80 backing pump (233 L s^{-1} for air at 0.2 Torr). Three possible sources of ionization are available within the source flow tube: a moveable electron impact source, a microwave discharge, and a hollow cathode discharge. Our experience indicates that the electron impact source (0.6 mm wide, 180 μm thick rhenium ribbon) is inclined to contaminate the flow tube and the ion sampling region more rapidly than either the microwave discharge or the hollow cathode sources. Reactant gases can be added to the source flow tube through either a moveable neutral inlet or one of two fixed inlets (Fig. 2). The length of the source flow tube is adjustable from 25 cm to up to 70 cm to facilitate the production of the optimum signal for each ion of interest. The carrier gas used in the source is generally helium although hydrogen and nitrogen have also been used. Typical operating pressures within the flowing afterglow ion source are between 0.2 and 1.0 Torr.

Ions generated in the FA source flow tube are carried in the buffer gas to a nose cone that is electrically insulated from its surrounds. This nose cone is floated at about +25 V for most cations in order to break down the plasma sheath and thus allow transmission of ions through the nose cone orifice. A small fraction of the ions are sampled through a 2-mm orifice in a 24-mm-diameter molybdenum disk at the nose cone apex. Ions transmitted through the nose cone are focused by a six-element lens assembly, which is mounted to the nose cone, into the ion selection quadrupole mass filter (Extrel model 7-270-9). The first element in this lens assembly is a conically shaped extractor lens with a 4-mm aperture (25.4-mm cone base diameter, 14.7 mm from apex to back plate), located 2 mm behind the nose cone orifice. The rectangular chamber housing the ion

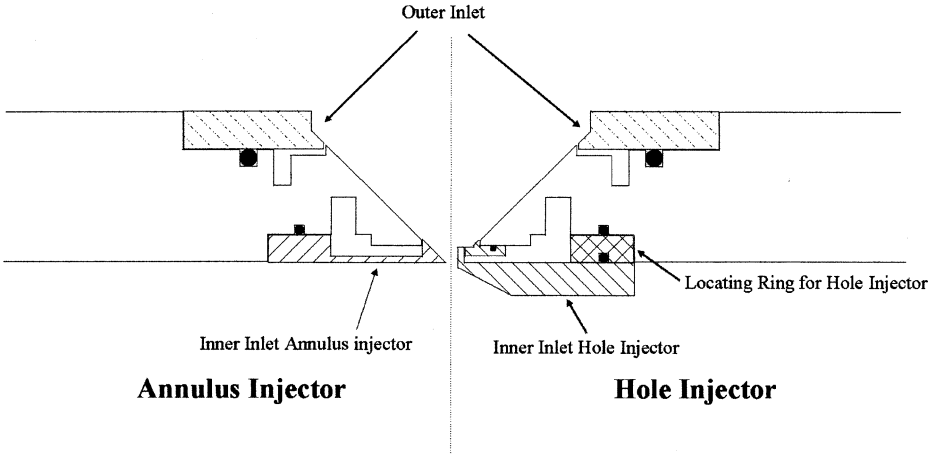

Fig. 3. Drawing of the Venturi injectors used in this work. The NOAA type II annulus injector is shown on the left side of the diagram and the interchangeable hole injector on the right. An outer annulus (37.1-mm diameter and 0.4-mm wide) is also present for both injectors.

selection quadrupole measures 40-cm long × 42-cm wide × 31-cm height and is pumped by a 25.4-cm oil diffusion pump (Varian VHS-400, 8000 L s^{-1}, air) backed by a Leybold-Heraeus D65B mechanical pump. A custom-built liquid nitrogen-cooled trap (holding time ~6 h) and a 25.4-cm Temescal pneumatic gate valve separate the chamber from the VHS-400 diffusion pump. The ion selection quadrupole is also differentially pumped by a 15-cm oil diffusion pump (Varian VHS-6, 2400 L s^{-1}, air) backed by a Leybold-Heraeus D30A mechanical pump. Typical operating pressures when the FA source and main reaction flow tubes are at 0.5 Torr pressure of helium are: ion selection chamber 1×10^{-5} Torr and quadrupole 1×10^{-6} Torr.

After ion mass selection in the quadrupole, the selected ions are focused by an Einzel lens system through a 2-mm orifice in the injector flange containing the Venturi inlet. Two different injector inlets were used in this study. A NOAA type II injector that has an inner annulus to create the Venturi effect and an outer annulus to reduce turbulence is the default inlet. We also constructed a "hole injector" such that it was interchangeable with the inner annulus section of the annulus injector flange and had exactly the same inlet area as the annulus injector (see Fig. 3). The details of each injector are summarized in Table 1. Each of the Venturi injectors, i.e. the "annulus" and the "hole" varieties, share the same outer annulus of dimensions (37.1-mm diameter and 0.4-mm wide). Because the "hole" injector inlet fits onto the same flange as the "annulus" injector, it allows a comparison between the two to be made under similar conditions.

The reaction flow tube used in the present FA/SIFT equipment is similar to that described earlier [10]. In brief, it consists of a 100-cm long, 7.3-cm i.d. tube

Table 1
Characteristics of the annulus and hole injectors used in this study

Type	Inner "orifice" dimensions/(mm)	Inner orifice area/$(mm)^2$	Inner orifice diameter/(mm)	Orifice-ion aperture separation
NOAA type II annulus[a]	Annulus width, 0.025	0.695	8.7	3.2
Hole[a]	12 hole, 0.25 diam.	0.695	4.25	3.0
Hole[b] (see [4])	12 hole, 0.20 diam.	0.4	11.1	~1.3

[a] Both injectors have the same outer annulus: 37.1-mm diameter and 0.4-mm wide.
[b] The dimensions of this injector are given for comparison and refer to the Pitt D injector recommended in [4] as having the best design.

connected via a bellows to the analyzer chamber. Three reactant gas inlets at different positions along the tube allow entry of known flow rates of reactant gases. The reaction flow tube is pumped by a high capacity Roots blower (JVE Model PMB-020, 570 L s^{-1} air at 0.1 Torr) backed by a JVE PKS-030 mechanical pump. Typical helium velocities are 8800 cm s^{-1} at 0.35 Torr increasing to 11 500 cm s^{-1} with the drift tube inserted.

A small fraction of the ion swarm is sampled through a 0.45-mm orifice in a molybdenum disk at the apex of the 126°, 15.2-cm OD nose cone situated at the end of the reaction flow tube. A new vacuum chamber has been constructed at the downstream end to improve the pumping efficiency in the analyzer quadrupole and ion detection region. The analyzer quadrupole and particle multiplier assembly are pumped by two 10-cm oil diffusion pumps (VHS-4, 1200 L s^{-1}) each separated from the analyzer chamber by gate valves and individual liquid nitrogen-cooled traps, and each backed by separate Welch Duoseal Model 1397 mechanical pumps. The typical operating pressure in the detector chamber when the reaction flow tube is at a pressure of 0.45 Torr helium is 1.2×10^{-5} Torr.

3. Results and discussion

3.1. Injector comparison

The two interchangeable injectors that are characterized in Table 1 were employed in the following comparisons. We have compared the performance of each injector (by varying the fraction of the helium buffer gas flowing through the inner inlet orifice) for their "Venturi" effect, their ion transmission efficiency (using O_2^+), their transmission of weakly bound cluster ions (using $H_3O^+ \cdot H_2O$), and finally the extent of isomeric transformation during the injection process (using $C_3H_5^+$ ions).

3.1.2. Venturi effect

The relative pumping efficiencies of "hole" type and "annulus" type injectors have been compared previously for isolated and separate injectors [5]. In the present test, using the interchangeable injectors described earlier, the ion selection chamber was isolated from all pumping stations. The pressures inside the chamber (P1) and the reaction flow tube (P2) were monitored, with P2 maintained at 0.35 Torr (helium) by mass flow controllers. The variation in the ratio (P2/P1) gives an indication of the extent of backstreaming from each injector into the ion selection chamber and is a measure of the Venturi effect of the injector. The results are shown in Fig. 4 for a total helium flow rate of 142 STP cm^3 s^{-1}. These results show much less backstreaming and a greater Venturi effect from the annulus injector ($P2/P1 \leq 7$) than from the hole injector ($P2/P1 \leq 1.38$), in keeping with the findings of Dupeyrat et al. with the injectors they tested [5]. It is also apparent that the degree of backstreaming for both types of injectors is markedly influenced by the relative amounts of gas passing through the Venturi (inner) orifice as opposed to the outer annulus. The other interesting feature is that there is less backstreaming at higher inner orifice fractional flows with the annulus injector whereas the reverse is true for the hole injector. In terms of performance, characteristics, and geometry the hole injector used here seems most similar to the hole injector designated Pitt E by FG [4], which exhibited similar behaviour.

3.1.3. Ion transmission

The variation in O_2^+ signal with the fraction of buffer gas passing through the inner orifice is shown in Fig. 5. It is evident that the annulus injector is less sensitive than the hole injector to the fraction of gas passing through it, which is in keeping with the lower backstreaming characteristics of this injector. In both injectors there is some correlation between the signal intensity and the extent of backstreaming that seems reasonable. For example, the maximum signal intensity for the hole injector occurs when 25% of the total gas flow passes through the injector, which correlates exactly with the position of minimum backstreaming in Fig. 4.

These results for signal intensity for the hole injector are different from those reported by Fishman

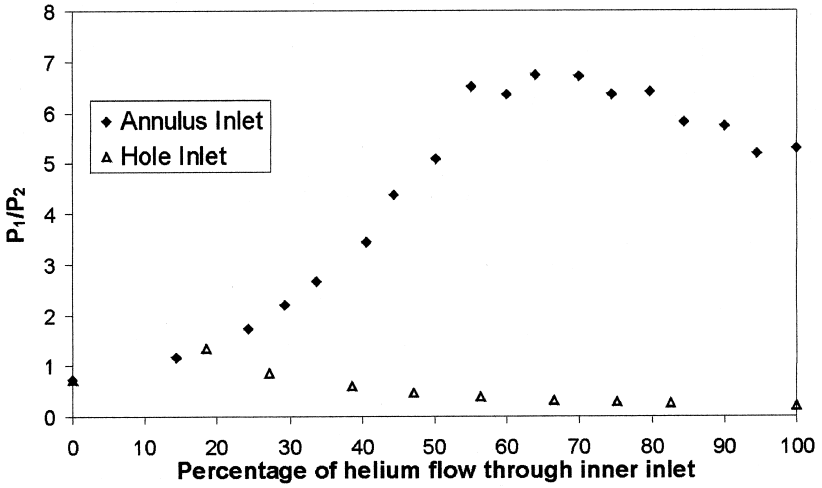

Fig. 4. The variation in the ratio (P_2/P_1) for the hole and annulus injectors described in Table 1, with the fraction of helium buffer gas passing through the injector. The total helium flow is 142 STP cm^3 s^{-1}.

and Grabowski for their hole injectors Pitt B, C, and D [4]. These have their maximum signal intensity for O^+ ions corresponding with maximum backstreaming when all the gas flow is directed through the inner holes. Enhancements in ion signals of up to around four to five times were found for both the present hole injector and those used in the FG study, except that in the present case, the maximum signal corresponded to 20% of the gas flow directed through the critical injector, rather than 100%. The absence of any apparent correlation in ion signal with backstreaming in the FG study indicates that the ion energy in their study was sufficient to counteract the scattering from increasing backstreaming.

The largest difference in design between the hole injector used in this work and those in the FG study lies in the hole circle diameter on which the twelve small holes are spaced. In this work the hole circle diameter of 4.25 mm (Table 1) was noticeably less than the equivalent measurement of 7.9 mm to 11.1 mm in the Pitt injectors (4). The ensuing turbulence at higher gas flows interacted with the ion beam in a

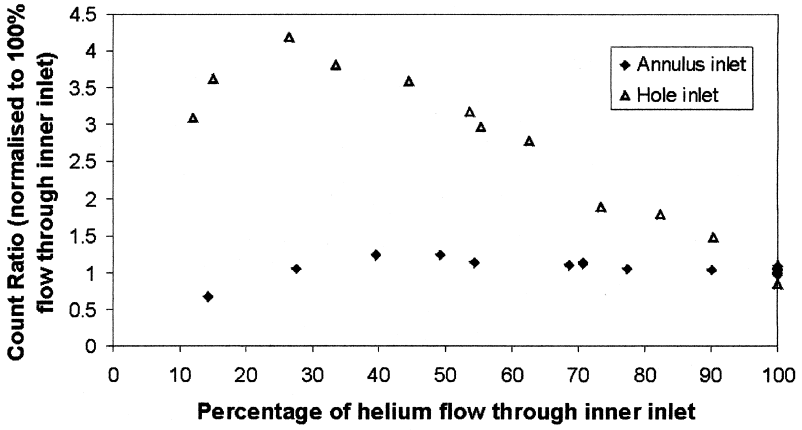

Fig. 5. The variation in O_2^+ signal with the fraction of helium buffer gas passing through the injector. The total helium flow is 142 STP cm^3 s^{-1}. For each curve the signal has been normalised to the average signal at 100% flow through each injector.

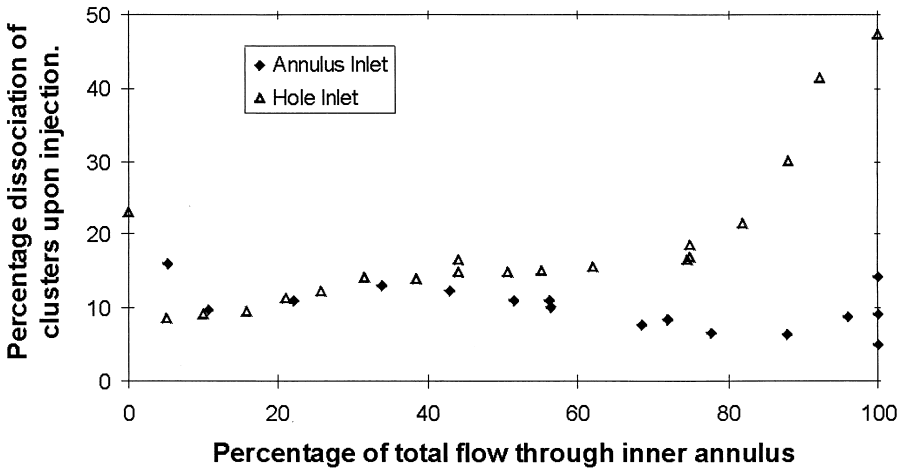

Fig. 6. The variation in dissociation of the ion $H_3O^+.H_2O$ to $H_3O^+ + H_2O$ with the fraction of helium buffer gas passing through the injector at a nose cone injection potential of +22.5 V. The total helium flow is 142 STP $cm^3\ s^{-1}$.

different manner from that where the inlets have a larger hole circle diameter.

3.1.4. Cluster ion dissociation

The $H_3O^+.H_2O$ ion was generated from water vapour in the FA source using a microwave discharge with helium as the buffer gas. After mass selection, the $H_3O^+.H_2O$ ion was focused into the ion entrance orifice on the injector flange. The extent of dissociation of the ion during the injection process was monitored by the analyzer quadrupole at the downstream end of the reaction flow tube by comparing H_3O^+ and cluster signals. The results for each injector are summarised in Fig. 6 for identical ion injection energies.

Both injectors are capable of transmitting the $H_3O^+.H_2O$ ion cluster with little breakup at low ion energies. What is quite different in the performance of the two injectors is the partitioning ratio of the carrier gas between inner and outer parts of the inlet system and its influence on cluster ion breakup. The best conditions (i.e. the conditions for minimum breakup) in the annulus injector were achieved when most of the helium carrier gas passed through the *inner* (Venturi) injector. However, in the hole injector, the optimum conditions were found when most of the helium passed through the *outer* annulus. The minimum amount of collisional dissociation thus corresponds to the maxima in the pumping efficiency curves for each injector (see Fig. 4). Under conditions where between 50% and 70% of the gas flow is directed through the inner annulus, the hole injector exhibits more fragmentation than does the annulus injector. At 50% flow, the extent of fragmentation is 50% larger for the hole injector and at 70% flow, it is a factor of 2.7 times larger.

On reflection these findings are not unexpected because the number of collisions between the injected ions and the bath gas will be influenced by the extent of backstreaming—a condition in which the carrier gas atoms exhibit a greater component of velocity opposed to the direction of ion travel. It is a little surprising in view of the moderate binding energy of the $H_3O^+.H_2O$ cluster ion (134 kJ mol^{-1} [12–14]) that the collisionally induced dissociation should be as large as it is.

We can draw some conclusions about the two types of injectors by combining these observations with the findings of Dupeyrat et al. [5]. It would appear that the hole injector used in this work forms “shock cells” in front of it. These cells are local pressure variations that deflect and dissociate the ions. By passing most of the gas load through the outer injector, the effect is reduced with a reduction in the degree of ion dissociation. In contrast, the annulus injector is less sensitive to the effect of carrier gas partitioning.

It was possible to inject $H_3O^+.H_2O$ with essentially no breakup using the *annulus* orifice at low FA nose cone voltages, and hence lower ion energies than those used in this experiment, but under these conditions the total number of counts had fallen from several thousand cps to less than 1000 cps. The same experience with this ion was reported by Williams et al. [15] who reported about 15% breakup from the $H_3O^+.H_2O$ ion in their study using a hole injector.

3.1.5. Isomerization upon injection

Energy barriers on the potential surface between isomeric ion structures are in some cases relatively small, so that the very process of injection of an ion may result in isomerization. The extent of isomerization may therefore provide a sensitive indicator of energy deposition during the injection process. The $C_3H_5^+$ ion is known to have two low energy forms. The global minimum on the $C_3H_5^+$ potential surface corresponds to the allyl structure, $CH_2CHCH_2^+$, with the 2-propenyl structure, $CH_3CCH_2^+$, 33 kJ mol^{-1} higher in energy [16]. The barrier between the two isomeric forms is calculated as being 75 kJ mol^{-1} above the 2-propenyl structure. It is possible to generate the 2-propenyl cation exclusively using proton transfer from a suitable protonated base, e.g. H_3O^+, to allene and propyne [16].

The isomeric structures of the $C_3H_5^+$ may be distinguished by their reactions with methanol [16,17]. We have reported earlier that when the 2-propenyl structure was formed in the FA source, it invariably rearranged to the allyl structure during the injection process [16]. The presence of the 2-propenyl structure was demonstrated by injecting H_3O^+ formed in the FA source into the SIFT reaction tube. Propyne was added at the first reaction inlet and the resultant $C_3H_5^+$ product ion reacts with methanol in a manner consistent with the 2-propenyl structure [16]. When this same reaction is performed in the FA source, the injected $C_3H_5^+$ ion reacts with methane in a manner consistent with the allyl structure. We injected the 2-propenyl ion formed in the FA source through both the hole and annulus injectors under a wide range of energies but were unsuccessful at all energies and with both injectors in preventing isomerization to the allyl structure from taking place.

3.2. H_3^+ + N reaction revisited

These experiments were carried out using the annulus injector only. We have earlier reported a moderately fast reaction between H_3^+ and atomic nitrogen with $k = 4.5 \times 10^{-10}$ cm^3 s^{-1} [18]

$$H_3^+ + N \rightarrow NH_2^+ + H \quad (1)$$

The experiments in that study were carried out using our original SIFT apparatus with a hydrogen carrier gas in order to avoid the formation of significant populations of vibrationally excited H_3^+ ($v > 0$) ions as well as large fractions of HeH^+ that can be formed when H_3^+ is injected into a helium carrier gas. Vibrational excitation of H_3^+ is known to occur in conventional ionization sources [19]. In our earlier work, Kr^+ was injected from a high pressure ion source into the hydrogen carrier gas and H_3^+ was subsequently formed by the reaction sequence:

$$Kr^+ + H_2 \rightarrow KrH^+ + H \quad (2)$$

$$KrH^+ + H_2 \rightarrow H_3^+ + Kr \quad (3)$$

The presence of vibrational excitation in H_3^+ can be detected from its reaction with Ar. No reaction occurs with H_3^+ ($v = 0$ or 1) but ArH^+ formation is exoergic for all vibrational levels except the three lowest [20]

$$H_3^+(v > 0, 1, 1) + Ar \rightarrow ArH^+ + H_2 \quad (4)$$

In our earlier study the evaluation of the rate coefficient for reaction (1) was difficult in that it was complicated by a simultaneous collision-rate proton transfer reaction between H_3^+ and N_2

$$H_3^+ + N_2 \rightarrow N_2H^+ + H_2 \quad (5)$$

Atomic nitrogen was made by microwave discharge on a mixture of He and N_2 and, typically, dissociation proceeded to the extent of between 1% and 1.5%. Consequently, over 98% of nitrogen was present in the form of molecular nitrogen and thus the rate coefficient for reaction (1) could not be measured in the usual way by monitoring the semilogarithmic decrease of H_3^+ with N atom flow. Instead, the rate coefficient was obtained from the observed ratio of products from the two reactions: N_2H^+ [reaction (5)]

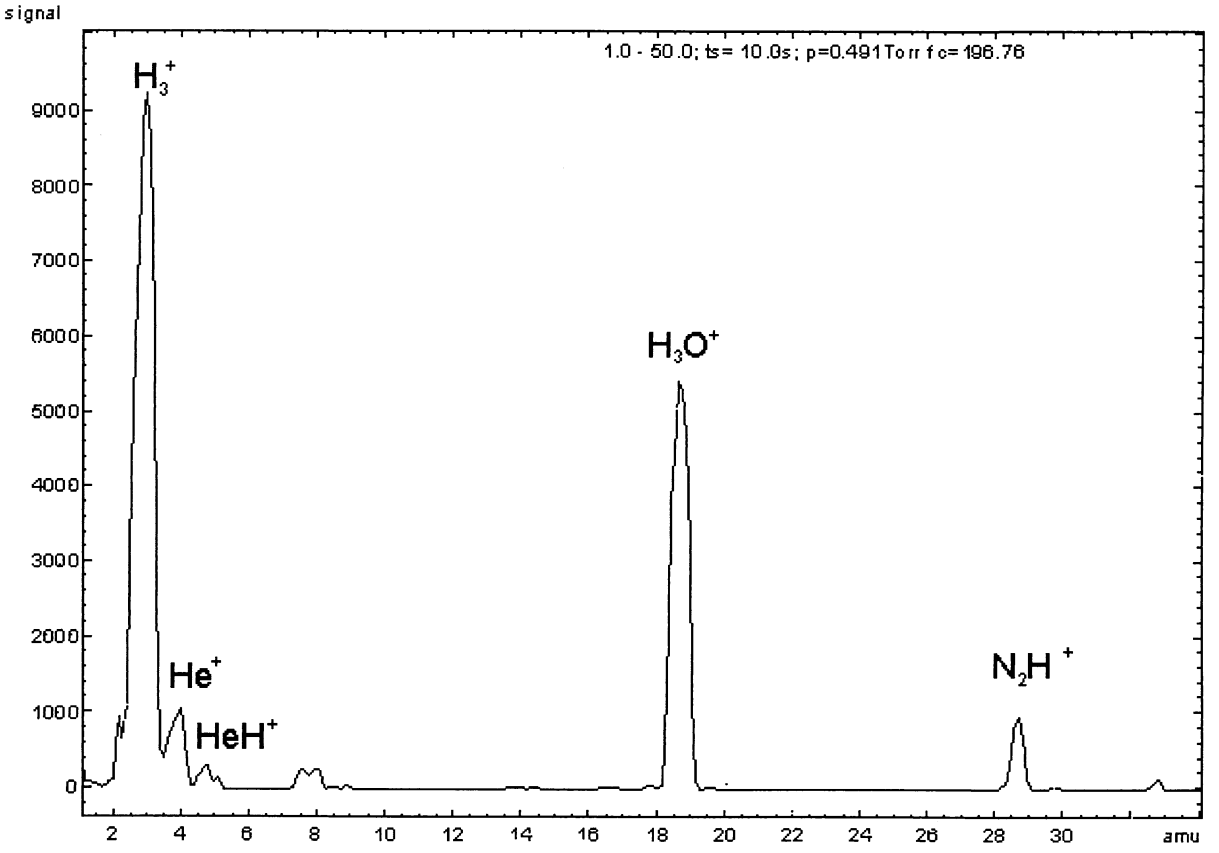

Fig. 7. The ions observed in the reaction flow tube after injecting H_3^+ formed from a microwave discharge in H_2 in the flowing afterglow source through the annulus injector into a helium carrier gas. Only small amounts of HeH^+ are present. The signal at 19 is H_3O^+ and 29 is N_2H^+ arising from trace impurities of H_2O and N_2, respectively. The trace shown is from a single scan of the downstream quadrupole over 10 s and shows all mass peaks between 1 and 50 Da.

and NH_2^+ [reaction (1)]. However, even this procedure had problems, as in the presence of excess H_2, NH_2^+ is converted to NH_4^+ via the sequence of reactions:

$$NH_2^+ + H_2 \rightarrow NH_3^+ + H \quad (6)$$

$$NH_3^+ + H_2 \rightarrow NH_4^+ + H \quad (7)$$

A better and more direct experimental procedure is to inject H_3^+ free from vibrational excitation into a *helium* carrier gas and to look for evidence of NH_2^+ formation. It is this experiment that we report here using the new FA/SIFT apparatus.

First, we must be able to inject workable signals of H_3^+, free from both significant vibrational excitation and the simultaneous formation of HeH^+, into a helium carrier gas. HeH^+ is observed when H_3^+ is injected at moderate energies into a helium buffer gas. This process [reaction (8)] is 245 kJ mol^{-1} endothermic and is a sensitive indicator of the injection energy in a SIFT

$$H_3^+ + He \rightarrow HeH^+ + H_2 \quad (8)$$

In our previous experiments when helium carrier was used, we were unable to inject H_3^+ free from appreciable amounts of HeH^+. We have now, however, been successful in achieving this with the modified FA source flow tube. A typical injection profile at low energies in the FA/SIFT experiment is shown in Fig. 7.

When we revisited reaction (1) using low energy H_3^+ formed from a hydrogen afterglow, we found no evidence whatsoever for the formation of NH_2^+ or

NH_3^+ under any conditions. We conclude, therefore, that reaction (1) does not occur. Based on our non-observation of any reaction products, we place an upper limit on the rate coefficient for reaction (1) at room temperature as $k < 5 \times 10^{-11}$ cm^3 s^{-1}. We now believe that in the earlier experiments [18], some of the H_2 in the flow tube may have contaminated the N_2 in the microwave discharge side arm, thus leading to trace amounts of NH_3 formed via neutral reaction chemistry. The signal we identified as NH_4^+ therefore probably came from proton transfer to NH_3 and not from reaction (1).

4. Concluding remarks

For a number of applications there is no great advantage to be obtained using the annulus injector instead of the hole injector. For strongly bound ions, although the performance of the annulus injector is better in most respects than the hole injector, it is not overwhelmingly so. The ease of construction and the lack of critical alignment features for the hole injector need to be balanced against the slightly better performance of the annulus. For small diameter hole circle injectors, such as the 4.25-mm hole circle used in this work, it is advantageous to bypass some of the buffer gas flow through a noncritical orifice. It was not possible to make an absolute comparison of ion signals between the two injectors because they could not be operated simultaneously and thus other factors such as ion source conditions could contribute to any observed differences. Typical ion densities for most ions (but not weakly bound ions) were around 400 ions cm^{-3} at the downstream end of the reaction flow tube for a helium pressure of 0.48 Torr. That ion density equates to 100 000 cps after transmission through the orifice in the downstream nose cone and the quadrupole filter and lens assembly. This number density appeared larger for the annulus injector than the hole injector but, again, not by more than a factor of two for the optimum injection conditions of each.

Both injectors achieved similar performance in the transmission of less strongly bound cluster ions—a rather surprising result in view of the smaller Venturi effect of the hole injector. The lower backstreaming characteristics of the annulus injector did, however, allow lower injection energies to be used without having to direct a significant fraction of the helium buffer gas flow through the outer annulus. It was necessary to direct a substantial amount (>40%) of the total helium flow through the outer annulus in the hole injector to achieve a reasonably low (10%) extent of dissociation in $H_3O^+.H_2O$. This is presumably due to the greater formation of shock cells with the hole injector and is probably also related to the small hole circle diameter used in the current hole inlet. That the injection procedure is of necessity an energetic process was demonstrated by the failure to inject the 2-propenyl ion, $CH_3CCH_2^+$, without isomerization occurring to the allyl structure, $CH_2CHCH_2^+$, during passage through the Venturi nozzle regardless of which injector was used.

Although it was not possible to compare the absolute ion signals for each injector directly, we were able to determine that there was little difference between them on the grounds of signal strength alone. It is apparent from the extent of fragmentation of less strongly bound ions that the annulus injector produced less fragmentation than the hole injector. On the other hand, no alignment was necessary with the hole injector, whereas the annulus injector takes typically an hour to adjust the inner critical annulus to a concentric position within the injector flange.

Finally, we were able to use the new FA source in the FA/SIFT apparatus to inject H_3^+ at sufficiently low energies to revisit the reaction of $H_3^+ + N$ using a helium bath gas. These experiments showed that no reaction occurred, which is in keeping with a recent evaluation and calculations of the potential surface and dynamics for this reaction [21].

Acknowledgements

The authors thank Drs. V. Bierbaum and C. DePuy for the generous provision of details and design characteristics of their FA/SIFT apparatus. We thank Dr. P.F. Wilson for assistance with the design of the new instrument and we also thank the Marsden Fund for financial support.

References

[1] F.C. Fehsenfeld, A.L. Schmeltekopf, P.D. Goldan, H.I. Schiff, E.E. Ferguson, J. Chem. Phys. 44 (1966) 4087.
[2] D. Smith, N.G. Adams, in Gas Phase Ion Chemistry, M.T. Bowers (Ed.), Academic, New York, 1979, Vol. 1, p. 1.
[3] N.G. Adams, D. Smith, Int. J. Mass Spectrom. Ion Phys. 21 (1976) 349.
[4] V.N. Fishman, J.J. Grabowski, Int. J. Mass Spectrom. 177 (1998) 175.
[5] G. Dupeyrat, B.E. Rowe, D.W. Fahey, D.L. Albritton, Int. J. Mass Spectrom. Ion Phys. 44 (1982) 1.
[6] G.I. Mackay, G.D. Vlachos, D.K. Bohme, H.I. Schiff, Int. J. Mass Spectrom. Ion Phys. 36 (1980) 259.
[7] G.K. King, M.M. Maricq, V.M. Bierbaum, C.H. DePuy, J. Am. Chem. Soc. 103 (1981) 7133.
[8] J.S. Knight, C.G. Freeman, M.J. McEwan, N.G. Adams, D. Smith, Int. J. Mass Spectrom. Ion Processes 67 (1985) 317.
[9] M.J. McEwan, in Advances in Gas Phase Ion Chemistry, N.G. Adams, L.M. Babcock (Eds.), J.A.I. Press, Greenwich, 1992, Vol. 1, p. 1.
[10] D.A. Fairley, G.B.I. Scott, D.B. Milligan, R.G.A.R. Maclagan, M.J. McEwan, Int. J. Mass Spectrom. Ion Processes 172 (1998) 77.
[11] J.M. Van Doren, S.E. Barlow, C.H. DePuy, V.M. Bierbaum, Int. J. Mass Spectrom. Ion Processes 81 (1987) 85.
[12] R.G. Keese, A.W. Castleman, J. Phys. Chem. Ref. Data 15 (1986) 1011.
[13] M. Mautner, C. Speller, J. Phys. Chem. 90 (1986) 6614.
[14] N.F. Dalleska, K. Honma, P.B. Armentrout, J. Am. Chem. Soc. 115 (1993) 12125.
[15] T.L. Williams, N.G. Adams, L.M. Babcock, Int. J. Mass Spectrom. Ion Processes 172 (1998) 149.
[16] D.A. Fairley, D.B. Milligan, L.M. Wheadon, C.G. Freeman, R.G.A.R. Maclagan, M.J. McEwan, Int. J. Mass Spectrom. 185–187 (1999) 253.
[17] D.H. Aue, W.R. Davidson, M.T. Bowers, J. Am. Chem. Soc. 98 (1976) 6700.
[18] G.B.I. Scott, D.A. Fairley, C.G. Freeman, M.J. McEwan, Chem. Phys. Lett. 269 (1997) 88.
[19] W.T. Huntress, M.T. Bowers, Int. J. Mass Spectrom. Ion Phys. 12 (1973) 1.
[20] D. Smith, P. Spanel, Chem. Phys. Lett. 211 (1993) 454.
[21] R.P.A. Bettens, M.A. Collins, J. Chem. Phys. 109 (1998) 9728.